Journal of Food Engineering 59 (2003) 191–198

JOURNAL OF FOOD ENGINEERING

www.elsevier.com/locate/jfoodeng

Predictive modelling of post-harvest quality evolution in perishables, applied to mushrooms

L.J.S. Lukasse *, J.J. Polderdijk

ATO, P.O. Box 17, 6700 AA Wageningen, The Netherlands

Received 7 June 2002; accepted 17 November 2002

Abstract

A large number of models on post-harvest quality evolution of perishables is available. Yet the number of applications is limited. The most common application is the comparison of shelf-life predictions for different constant temperature scenarios.

Application of post-harvest quality evolution models for perishables in evaluation of cold-*chains* (non-constant temperatures) and in model predictive control (MPC) poses specific requirements to the models: predictive, causal, stable, irreversible models are required that are valid for non-constant temperatures.

In this paper a modelling methodology is presented in which the class of permitted models is limited by the above requirements. The methodology is used to develop a post-harvest mushroom quality evolution model.

The resulting model fits well to experimental data collected for mushrooms from three different growers. The model is suitable for use in MPC and the evaluation of cold-*chains* with any possibly occurring temperature trajectory. No such model is currently available in the literature.

Keywords: Identification; Methodology; Irreversibility; Colour evolution; Fruits; Vegetables

1. Introduction

A large number of models on post-harvest quality evolution of perishables (mainly fruits and vegetables) has been developed in the past (e.g. Hertog, Tijskens, & Hak, 1997; Nicolaï, van Impe, Martens, & de Baerdemaeker, 1995; Schouten & van Kooten, 1998; Tijskens, Otma, & van Kooten, 1998; Tijskens, Rodis, Hertog, Kalantzi, & van Dijk, 1998; Vankerschaver, Willocx, Smout, Hendrickx, & Tobback, 1996). Until now the number of applications of these models has been limited. The most common application is the comparison of shelf-life predictions as a function of different temperature scenarios, e.g. for the evaluation of cold-chains for storage and distribution of harvested crops. Usually these simulations are limited to constant temperatures.

Potential application areas for post-harvest quality evolution models are the evaluation of real cold-chains (non-constant temperatures) and the use of these models in model predictive control (MPC). Besides evaluating the effect of existing climatic conditions, the models can be used in conjunction with the theory of optimal control (Lewis, 1986) in order to optimise the course of climatic conditions during storage and distribution in view of objectives for crop quality evolution. Model predictive control is a natural tool to implement this optimal trajectory in practice. Only a limited number of applications of quality evolution models in MPC is available now (e.g. Trelea, Trystram, & Courtois, 1997; Verdijck & Lukasse, 2000; Verdijck, Weiss, & Preisig, 1999).

Both the use in MPC and in real cold-chains poses new requirements to the models. Models are required that

1. *predict* the future quality evolution as a function of the current state variables and the course of future climate conditions,
2. are *causal* (current quality evolution is independent of future conditions),
3. are valid for *non-constant* temperatures,

* Corresponding author. Tel.: +31-317-475301/475029; fax: +31-317-475347.
E-mail address: l.j.s.lukasse@ato.wag-ur.nl (L.J.S. Lukasse).
URL: http://www.ato.wageningen-ur.nl/.

0260-8774/03/$ - see front matter © 2003 Elsevier Science Ltd. All rights reserved.
doi:10.1016/S0260-8774(02)00458-2

4. accommodate the typical *irreversible* quality evolution of crops in the post-harvest stage,
5. are *stable* in forward time.

This paper presents a modelling methodology in which the class of permitted models is limited by the five above requirements. Although the development of a model for post-harvest mushroom quality evolution serves as an example, the resulting model itself will be useful as well. It may especially turn out to be useful in cold-chain evaluation. No such model is currently available in the literature.

2. Mushroom quality: background

The post-harvest quality evolution of mushrooms is always appreciated as quality degradation, this in contrast with e.g. banana ripening. Under ideal climatic conditions the post-harvest life of mushrooms is limited to at most 10 days, due to their fast quality devaluation. Quality evolution is predominantly affected by temperature. As an example the post-harvest life reduces from about 9 days at 2 °C to 3 days at 18 °C (this paper).

The short shelf-life in combination with the strong temperature sensitivity necessitates the thorough evaluation of non-optimalities in cold-chains in order to maximise shelf-life. A model describing quality evolution and fulfilling the five prerequisites in the introduction is an indispensable tool in evaluating any possible cold-chain.

In its pure definition a product's quality is the user's appreciation of the observed quality attributes. The user's appreciation depends on many other factors than just the quality attributes, but that is out of the scope of this paper. Overall mushroom quality is mainly composed of three quality attributes: colour, stipe length and hat opening. Consumers in continental Europe prefer white mushrooms. Also appreciated, but less important, are a closed hat and a short stipe. Hence continental European consumers prefer mushrooms in the condition in which mushrooms are harvested.

After harvest the mushroom colour gradually changes from white to brown, while the growth of stipe and hat just continues. The hat growth results in gradual opening of the mushroom hat. The evolution of the three quality attributes occurs at similar time scales. Hence the evolution of all three quality attributes as a function of temperature is relevant to the evaluation of cold-chains and should therefore be incorporated in the quality evolution model.

In this paper mushroom quality is defined as a three-dimensional vector:

$$\mathbf{y} = [\text{colour}, \ \text{stipe length}, \ \text{hat opening}]^{\mathrm{T}}$$

The quality $\mathbf{y}$ is visually determined and expressed in score values on a discrete scale from 0 to 5. The relation between visually observed quality and attributed score value is described in Table 1. Usually mushrooms are no longer acceptable to retailers, once one of the quality attributes reaches value three.

3. Methodology: experimental design and modelling procedure

1. The first step in identification of quality evolution dynamics is the design of an identification experiment on the basis of (often heuristic) a priori knowledge and collection of experimental data.

After having collected the identification data the actual modelling process starts:

2. Make the collected data suitable for fitting the model to the data by reducing the number of fives in an observed time series to at most one. For example an observed time series [0 3 5 5 5] (Table 1) is shortened to [0 3 5]. Shortening the time series avoids an undesired overweighing of low qualities in the data-fitting process. Moreover once a quality attribute has reached value five, it has reached the end of the measuring scale, although the quality may still further deteriorate. Hence in a sequence of fives only the first contains meaningful information.
3. Formulate the initial mathematical model. This model exists of available mechanistic knowledge, cast in a mathematical model with partly unknown parameter values.

Table 1
Relation between visible quality of a batch of mushrooms and attributed score value

Score value	Colour	Stipe length	Hat opening
0	White	No growth	Completely closed
1	Very slight colourization	First sign of growth	First sign of hat growth at stipe
2	Some colourization	Some growth	10–20% of mushrooms per batch show first signs of hat opening
3	Moderate	Clear growth of some stipes	20–50% of mushrooms per basket show first signs of hat opening
4	Brown	Clear growth of most stipes	Most hats open
5	Strong brown colour	Strong growth	All hats completely open

4. Estimate the unknown model parameters (see immediately below this stepwise procedure for more details).
5. Accept/reject the new model on the basis of a trade-off between goodness-of-fit ('sse' in Eq. (1)), number of model parameters and model structure.
6. Try to improve the model by modifying the model structure. Selecting a new model structure is a creative process using
   - the observed correlation in data-model misfit,
   - mechanistic knowledge of the product's quality evolution characteristics,
   - the five prerequisites mentioned in the introduction.

After having modified the model structure, the modelling procedure starts again from step 4.

7. Terminate the modelling cycle if an acceptable balance has been achieved between goodness-of-fit, number of parameters and model structure.

The general parameter estimation problem (step 4 in the procedure) is formulated as a non-linear optimisation problem. This non-linear optimisation problem takes the form:

$$\min_{\mathbf{p}} \text{sse} = \sum (y_k - \hat{y}_k(\mathbf{p}))^2 \tag{1}$$

subject to the non-linear system dynamics

$$\begin{aligned} \dot{\mathbf{x}}_k &= f(\mathbf{x}_k, T, \mathbf{p}) \quad \text{with } \mathbf{x}_0 = \mathbf{x}_0(\mathbf{p}) \\ y_k &= h(\mathbf{x}_k) \end{aligned} \tag{2}$$

where $f(\cdot)$ is the (possibly non-linear) state equation; $h(\cdot)$ is the (possibly non-linear) output equation; k is the time instant in days; $\mathbf{p}$ is the vector of model parameters in Eq. (2); 'sse' is the sum of squared errors between measurements and model outputs; T is the temperature in °C; $\mathbf{x}_0$ is the initial value of model state vector $\mathbf{x}$, during parameter estimation some of the $\mathbf{x}_0$-elements may be treated as model parameters $\mathbf{p}$; $\mathbf{x}_k$ is the model state vector at time k; y_k is a measured quality attribute at time k; and $\hat{y}_k(\mathbf{p})$ is a model estimate of quality attribute y at time k on the basis of model parameter values $\mathbf{p}$.

In case the parameters are identifiable from the data, the above non-linear optimisation problem is straightforwardly solved by programming it in MATLAB 5.3, using the function *lsqnonlin* in MATLAB's optimisation toolbox version 2.0.

In the next two sections the above stepwise identification procedure (steps 1–7) is applied to mushroom quality evolution. The next section discusses the collection of experimental data (step 1). The modelling of the three quality attributes is decoupled in order to reduce the problem's complexity. For each quality attribute the modelling procedure (steps 2–7) is followed. Application of the modelling procedure (steps 2–7) to the mushroom's quality attribute 'colour evolution' is presented in detail in the section 'Modelling colour evolution'. For the quality attributes stipe elongation and hat opening, the same procedure was followed. Therefore only the resulting models for stipe elongation and hat opening are presented, and not the detailed procedure.

4. Materials and methods for experimental identification of mushroom quality evolution

Experiments were carried out to identify the behaviour of mushroom quality evolution (step 1). For the experiment, mushrooms in 250 g baskets from three different growers were transported to ATO within one day after harvest. A quicker start of the experiments was impossible for practical reasons.

In this stage optimal experimental design by mathematical optimisation of non-constant temperature trajectories, like e.g. in Munack (1989), would make little sense due to large uncertainty in prior knowledge. Moreover the sharing of refrigerated cells with other experiments imposes fierce constraints. Therefore design of the experiment is solely based on practical experience.

The mushrooms were stored in refrigerated cells at ATO controlled at 2, 7, 12 and 18 °C. The range 2–18 °C is regarded as the practically relevant range. Much lower than 2 °C does not occur in practice in order to avoid freezing. The concrete temperature of 18 °C is a slightly arbitrary upper limit; it is just a high temperature causing fast quality evolution, which should be avoided in practice. The exact values of 2, 7, 12 and 18 °C were partly imposed by the fact that refrigerated cells had to be shared with other experiments.

During the experiment the three mushroom quality attributes colour, stipe length and hat opening were manually evaluated by a mushroom expert on intervals of 1–3 days, depending on storage temperature. One evaluation at one temperature is performed for four baskets from each grower, resulting in 12 (3 growers × 4 baskets per grower) measurements per measurement instant per quality attribute for each temperature. Evaluated mushrooms were immediately discarded. The use of new mushrooms for each evaluation is necessary to exclude the negative effect of manual contact on mushroom colour from the data set.

The resulting overall data set exists of three sets of measurement data like shown in Fig. 1 (three quality attributes). Note that in each subplot at each sampling instant there are four measurements per grower, not all of them are visible in Fig. 1 because they coincide.

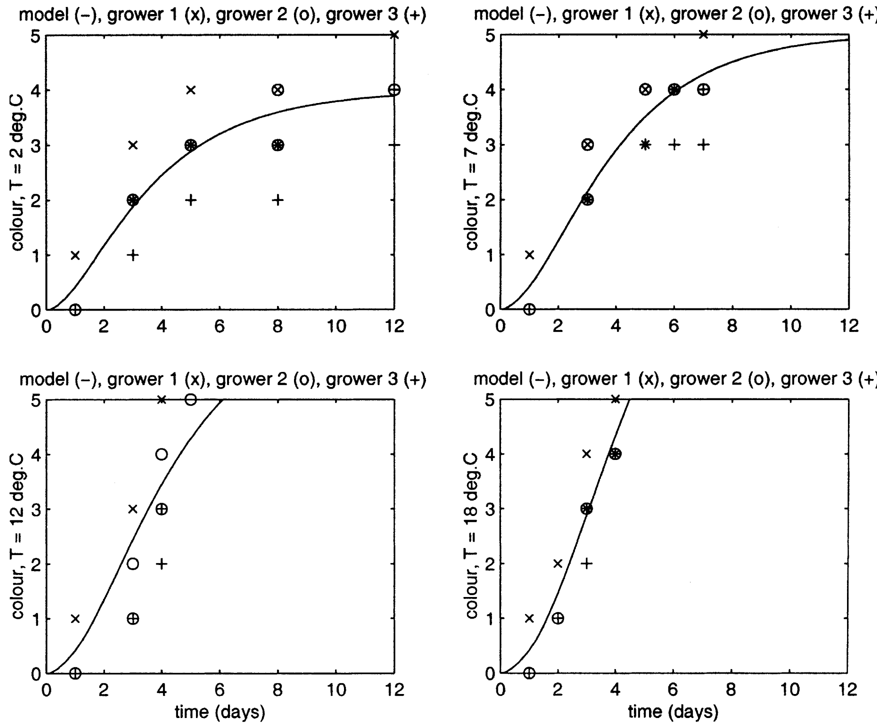

Fig. 1. Measured and simulated colour evolution at different temperatures.

5. Modelling colour evolution

The collected data (Fig. 1) contains several time series with multiple fives at the end. First all these time series are shortened till only 1 five remains at the end (step 2).

Step 3 in the procedure is the formulation of a mathematical model based on available mechanistic knowledge. This initial model is a slight modification of the model formulated in Tijskens (1990) and is given by

$$\begin{aligned} \dot{x}_1 &= -k_{ppo}x_1 && \text{with } x_1(t_0) = x_{1,0} \\ \dot{x}_2 &= k_{ppo}x_1 - k_{brown}x_2 && \text{with } x_2(t_0) = 0 \\ \dot{x}_3 &= k_{brown}x_2 + k_{TDF}T && \text{with } x_3(t_0) = 0 \\ y &= x_3 \end{aligned} \tag{3}$$

where x_1 is the polyphenol oxidase (PPO) precursor concentration; $\dot{x}_i = dx_i/dt$ is the time derivative of x_i; $x_{1,0}$ is the unknown x_1 concentration at harvest time t_0; x_2 is the PPO concentration; x_3 is the chinons concentration; y is the colour level; k_{ppo} is the rate at which x_1 is converted into x_2; k_{brown} is the rate at which x_2 is converted into x_3; and k_{TDF} is the constant introduced to model the temperature dependence of final value of y.

The physical basis for the above equations is the knowledge that the following chemical reactions take place in harvested mushrooms (Tijskens, 1990):

$$\text{P} \xrightarrow{k_{ppo}} \text{PPO}$$

$$\text{PPO} + \text{DP} \xrightarrow{k_{brown}} \text{Chinon}$$

The reaction rates k_{ppo} and k_{brown} are assumed independent of the reactant concentrations, and DP (diphenols) is assumed abundantly available. An unknown precursor P is supposed to convert into PPO. The enzyme PPO stimulates the conversion of DP into chinons. Chinons are known to polymerise rapidly into brown colouring agents. Eq. (3) assumes instantaneous conversion of chinons into brown colouring agents. The term $k_{TDF}T$ in Eq. $(3)_3$ reflects the empirically known small temperature dependence of the final mushroom colour y, the mechanism behind this temperature dependence is not yet understood.

In Tijskens (1990) the temperature dependence of rates k_{ppo} and k_{brown} in Eq. (3) is described by the generally used Arrhenius law (Bastin & Dochain, 1990)

$$k = k_{ref} \exp\left[E_A\left(\frac{1}{T_{ref} + 273} - \frac{1}{T + 273}\right)\right] \tag{4}$$

where E_A is the energy of activation; T_{ref} is the reference temperature in °C; and k_{ref} is the rate k at reference temperature T_{ref}.

Hence the unknown parameters in the initial physical model are: $\mathbf{p} = [k_{brown,ref}, k_{ppo,ref}, E_{A,brown}, E_{A,ppo}, T_{ref}, k_{TDF}, x_{1,0}]$.

The physical model, Eqs. (3) and (4), does not meet the requirement of irreversibility (see introduction): the term $k_{TDF}T$ enables white colouring of brown mushrooms by reducing T, which is physically impossible. Therefore an alternative empirical model structure is postulated that does accommodate the temperature dependence of final mushroom colour y and fulfils the prerequisite of irreversibility. Such a candidate model structure is

$$\begin{aligned} \dot{x}_1 &= -k_{\text{ppo}} x_1 && \text{with } x_1(t_0) = x_{1,0} \\ \dot{x}_2 &= k_{\text{ppo}} x_1 - (k_{\text{brown}} + k_{\text{loss}}) x_2 && \text{with } x_2(t_0) = 0 \\ \dot{x}_3 &= k_{\text{brown}} x_2 && \text{with } x_3(t_0) = 0 \\ y &= x_3 \end{aligned} \tag{5}$$

with k_{ppo}, k_{brown} and k_{loss} temperature-dependent rates. A temperature-dependent k_{loss} can make x_2 disappear and hence the model structure is sufficiently rich to make final mushroom colour y temperature-dependent. Yet Eq. (5) meets all requirements mentioned in the introduction. Physical justification of the term k_{loss} is that x_2 (PPO) might be depleted by other mechanisms.

In the parameter estimation process (step 4) first the vector $\mathbf{p} = [k_{\text{ppo}}(T)\ k_{\text{brown}}(T)\ k_{\text{loss}}(T)\ x_{1,0}]$ is optimised per temperature (four separate estimation problems), with the model solely existing of Eq. (5). In the four estimated parameter vectors the differences mainly occur in $k_{\text{ppo}}(T)$, $k_{\text{brown}}(T)$ and $k_{\text{loss}}(T)$. In all four estimated parameter vectors $x_{1,0}$ takes large values between 60 and 80. Therefore in the overall estimation problem $x_{1,0}$ is treated as a constant: $x_{1,0} = 70$.

Solving the overall estimation problem for the model in Eqs. (4) and (5) (step 4), using the non-linear Arrhenius law, is complicated by poor parameter convergence. Moreover this *non-linear* temperature dependence of reaction rates is not immediately visible from the estimated k-values per temperature. Therefore the Arrhenius law is replaced by a linear temperature dependence (step 6):

$$\begin{aligned} k_{\text{ppo}} &= k_{\text{ppo},1} T + k_{\text{ppo},0} && \text{with } T \text{ in } ^\circ\text{C} \\ k_{\text{loss}} &= k_{\text{loss},1} T + k_{\text{loss},0} && \text{with } T \text{ in } ^\circ\text{C} \\ k_{\text{brown}} &= k_{\text{brown},1} T + k_{\text{brown},0} && \text{with } T \text{ in } ^\circ\text{C} \end{aligned} \tag{6}$$

In fitting the parameters of this model (Eqs. (5) and (6)) no convergence problem occurs and the 'sse' even reduces as compared to using Arrhenius law. The result is $[k_{\text{loss},0}\ k_{\text{loss},1}\ k_{\text{brown},0}\ k_{\text{brown},1}\ k_{\text{ppo},0}\ k_{\text{ppo},1}] = [0.9528, -0.0417, 0.0547, -0.0005, 0.3177, 0.0125]$ with sse = 82.3994 (step 4). The estimated $k_{\text{brown},1}$ appears insignificant and is therefore fixed at 0 (step 6). The new estimation result then is: $[k_{\text{loss},0}\ k_{\text{loss},1}\ k_{\text{brown},0}\ k_{\text{ppo},0}\ k_{\text{ppo},1}] = [0.8912, -0.0361, 0.0505, 0.3392, 0.0073]$ with sse = 82.4795 (step 4). Reducing the number of parameters at the expense of a minor increase of 'sse' is regarded as an improvement (step 5).

It is tried to further improve the fit by making the rate k_{brown} a function of both T and x_2 (step 6), using the common Monod kinetics (Bastin & Dochain, 1990):

$$k_{\text{brown}} = (k_{\text{brown},1} T + k_{\text{brown},0}) \frac{x_2}{k_{\text{half}} + x_2} \tag{7}$$

The fit results for this model are: $[k_{\text{loss},0}\ k_{\text{loss},1}\ k_{\text{brown},0}\ k_{\text{brown},1}\ k\ \ \text{ppo},0\ k_{\text{ppo},1}\ k_{\text{half}}] = [0.9719, 0.0431, 47.3720, -0.4126, 0.3156, 0.0123, 840.39]$ with sse = 82.4335 (step 4). Hence, adding Monod kinetics increases the number of parameters and adds a non-linearity to the model, while the model fit hardly improves. Therefore this model is rejected (step 5) and the model existing of Eqs. (5) and (6) remains the best available model.

The linear temperature dependence of the reaction rates (Eq. (6)) is fine for the temperature range in which the experimental data have been collected (2–18 °C). However when the model is used for simulating the quality evolution at lower temperatures the model may violate the requirements 4 and 5 in the introduction by showing unstable and reversible behaviour, as the rates may become negative. This shortcoming is easily removed by truncating the linear dependence (step 6):

$$\begin{aligned} k_{\text{ppo}} &= \max(k_{\text{ppo},1} T + k_{\text{ppo},0}; 0) && \text{with } T \text{ in } ^\circ\text{C} \\ k_{\text{loss}} &= \max(k_{\text{loss},1} T + k_{\text{loss},0}; 0) && \text{with } T \text{ in } ^\circ\text{C} \\ k_{\text{brown}} &= \max(k_{\text{brown},1} T + k_{\text{brown},0}; 0) && \text{with } T \text{ in } ^\circ\text{C} \end{aligned} \tag{8}$$

This truncation does not effect the model outcomes in the temperature range 2–18 °C, and therefore has no effect on the goodness-of-fit.

The finally accepted colour evolution model (step 7) exists of Eqs. (5) and (8) with

$$\begin{aligned} x_{1,0} &= 70 \\ k_{\text{ppo},0} &= 0.3392\ \text{day}^{-1} \\ k_{\text{ppo},1} &= 0.0073\ \text{day}^{-1}\ ^\circ\text{C}^{-1} \\ k_{\text{loss},0} &= 0.8912\ \text{day}^{-1} \\ k_{\text{loss},1} &= -0.0361\ \text{day}^{-1}\ ^\circ\text{C}^{-1} \\ k_{\text{brown},0} &= 0.0505\ \text{day}^{-1} \\ k_{\text{brown},1} &= 0\ \text{day}^{-1}\ ^\circ\text{C}^{-1} \end{aligned}$$

See Fig. 1 for a graphical illustration of the model fit.

6. Stipe elongation and hat opening

For stipe elongation and hat opening the same modelling procedure has been followed as mentioned before. Hence only the final results are presented in this section.

Stipe elongation is modelled as

$$\begin{aligned} \dot{x}_1 &= -k_{\text{pre}} x_1 && \text{with } x_1(t_0) = 70 \\ \dot{x}_2 &= k_{\text{pre}} x_1 - (k_{\text{stipe}} + k_{\text{loss}}) x_2 && \text{with } x_2(t_0) = 0 \\ \dot{x}_3 &= k_{\text{stipe}} x_2 && \text{with } x_3(t_0) = 0 \end{aligned} \tag{9}$$

where x_1 is the initial capacity for stipe elongation; x_2 is the stipe elongation precursor; x_3 is the stipe length (on scale 0–5, see Table 1); and $\dot{x}_3$ is the increase of stipe length per day.

With the rates k_{pre}, k_{loss} and k_{stipe} being temperature dependent according to

$$
\begin{aligned}
k_{pre} &= \max(k_{pre,1}T + k_{pre,0}; 0) && \text{with } T \text{ in °C} \\
k_{loss} &= \max(k_{loss,1}T + k_{loss,0}; 0) && \text{with } T \text{ in °C} \\
k_{stipe} &= \max(k_{stipe,1}T + k_{stipe,0}; 0) && \text{with } T \text{ in °C}
\end{aligned}
\quad (10)
$$

where

$k_{pre,0} = -0.1266\ \text{day}^{-1}$
$k_{pre,1} = 0.1825\ \text{day}^{-1}\ °\text{C}^{-1}$
$k_{loss,0} = 0.7802\ \text{day}^{-1}$
$k_{loss,1} = -0.0269\ \text{day}^{-1}\ °\text{C}^{-1}$
$k_{stipe,0} = 0.0435\ \text{day}^{-1}$
$k_{stipe,1} = 0\ \text{day}^{-1}\ °\text{C}^{-1}$

The truncation of the rates in Eq. (10) is in similarity with the truncation used for colour evolution (Eq. (8)). See Fig. 2 for a graphical illustration of the model fit.

Hat opening is modelled as

$$
\begin{aligned}
\dot{x}_1 &= -k_{pre}x_1 && \text{with } x_1(t_0) = 70 \\
\dot{x}_2 &= k_{pre}x_1 - (k_{hat} + k_{loss})x_2 && \text{with } x_2(t_0) = 0 \\
\dot{x}_3 &= k_{hat}x_2 && \text{with } x_3(t_0) = 0
\end{aligned}
\quad (11)
$$

where x_1 is the initial capacity for hat opening; x_2 is the hat opening precursor; x_3 is the hat opening (on scale 0–5, see Table 1); and $\dot{x}_3$ is the change of hat opening per day.

With the rates k_{pre}, k_{loss} and k_{hat} being temperature dependent according to

$$
\begin{aligned}
k_{pre} &= \max(k_{pre,1}T + k_{pre,0}; 0) && \text{with } T \text{ in °C} \\
k_{loss} &= \max(k_{loss,1}T + k_{loss,0}; 0) && \text{with } T \text{ in °C} \\
k_{hat} &= \max(k_{hat,1}T + k_{hat,0}; 0) && \text{with } T \text{ in °C}
\end{aligned}
\quad (12)
$$

where

$k_{pre,0} = 0.3107\ \text{day}^{-1}$
$k_{pre,1} = 0.0480\ \text{day}^{-1}\ °\text{C}^{-1}$
$k_{loss,0} = 0.5547\ \text{day}^{-1}$
$k_{loss,1} = 0\ \text{day}^{-1}\ °\text{C}^{-1}$
$k_{hat,0} = 0.0147\ \text{day}^{-1}$
$k_{hat,1} = 0.0035\ \text{day}^{-1}\ °\text{C}^{-1}$

The truncation of the rates in Eq. (12) is in similarity with the truncation used for colour evolution (Eq. (8)). See Fig. 3 for a graphical illustration of the model fit.

7. Discussion

For some products significant differences in quality evolution are observed between different batches. The phenomenon is usually indicated as biological variation (e.g. Tijskens, Hertog, van Kooten, & Simcic, 1999). To some extent these differences were also observed in this paper. In Fig. 1 grower 3 (+) always has the best quality, while grower 1 (x) has the worst quality. The most likely explanation for the differences in quality evolution are the differences in initial state, while the actual reaction kinetics are the same (like also stated by Tijskens et al., 1999). The observed differences in quality evolution between batches illustrate the need for improved measurement techniques in order to reduce the unobserved subspace (initial concentrations).

The resulting overall model has a rather high dimension (**x** has dimension 9, Eqs. (5), (9) and (11)). It

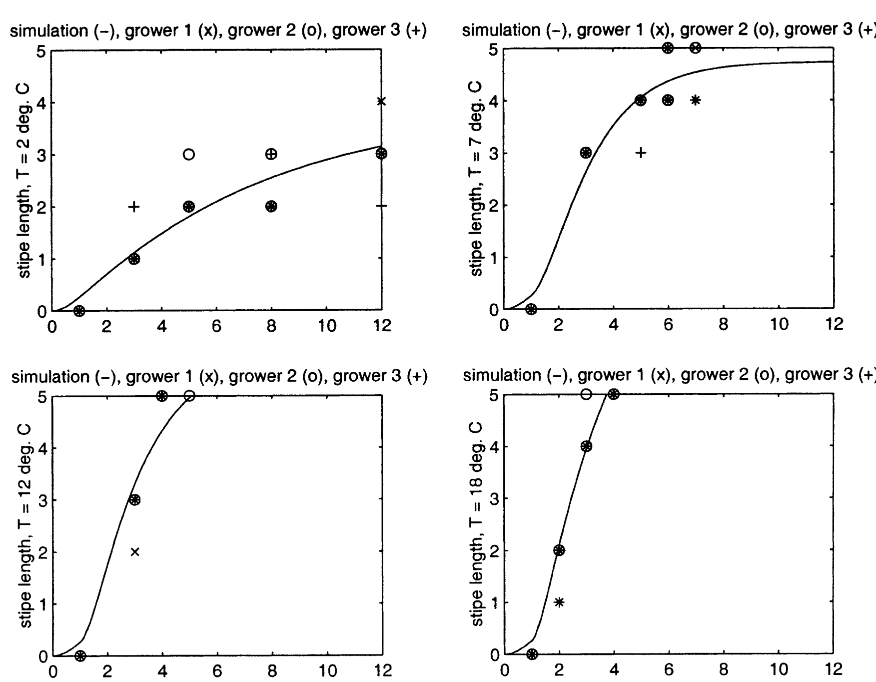

Fig. 2. Measured and simulated stipe elongation at different temperatures.

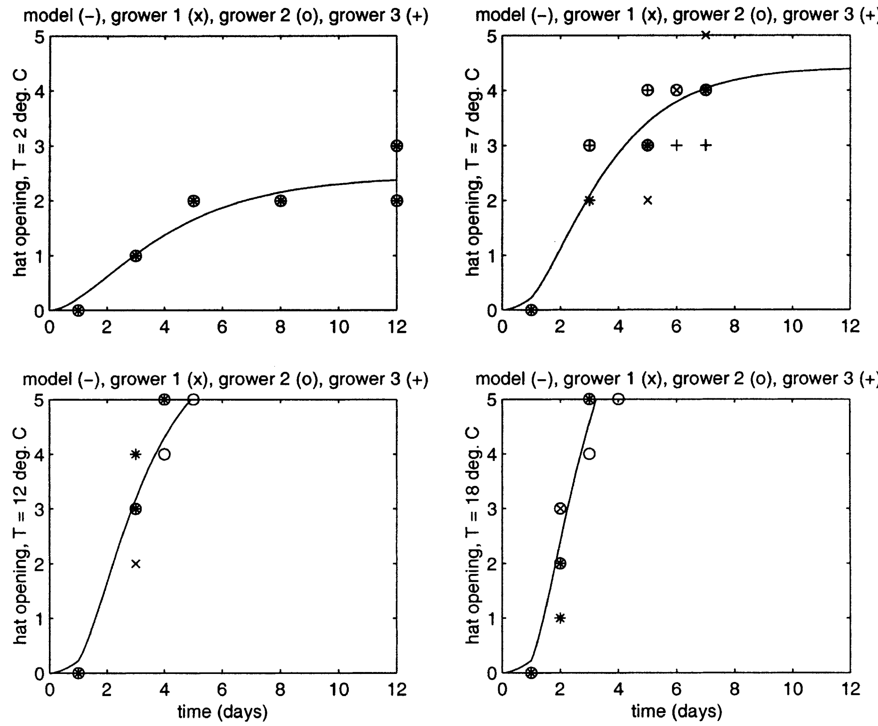

Fig. 3. Measured and simulated hat opening at different temperatures.

would be interesting to investigate whether coupling of the three submodels can reduce the model dimension. For example, is it possible to reduce the model dimension by creating a direct coupling between stipe elongation and hat opening?

It is known that draft (wind) has an adverse effect on colour evolution. This effect is not yet incorporated in the quality evolution model due to lack of both experimental data and mechanistic understanding.

8. Conclusions

A methodology for modelling quality evolution of perishables has been presented. The use of the methodology has been demonstrated for mushroom quality evolution. Using the methodology and the five requirements (given in the section 'Introduction') is straightforward and leads to quality evolution models that predict the quality evolution for any temperature trajectory.

The developed model fulfils the five criteria listed in the introduction and fits reasonably well to the data (Figs. 1–3). All observed quality evolutions, at different temperatures and from different growers, are to a large extent explained with only one general model. This makes the model suitable for use in MPC and the evaluation of cold-chains with any possibly occurring temperature trajectory. Moreover the model may be used to compute the optimal temperature trajectory for more accurate identification of quality evolution dynamics or in view of specific quality evolution objectives.

Acknowledgements

We thank our colleague L.L.M. Tijskens for his fruitful discussions and Produktschap Tuinbouw for its financial support of the research project.

References

Bastin, G., & Dochain, D. (1990). *On-line estimation and adaptive control of bioreactors*. Amsterdam, The Netherlands: Elsevier Science Publisher.

Hertog, M. L. A. T. M., Tijskens, L. M. M., & Hak, P. S. (1997). The effects of temperature and senescence on the accumulation of reducing sugars during storage of potato (*Solanum tuberosum* L.) tubers: A mathematical model. *Postharvest Biology & Technology, 10*, 67–79.

Lewis, F. L. (1986). *Optimal control*. New York: John Wiley & Sons.

Munack, A. (1989). Optimal feeding strategy for identification of Monod-type models by fed-batch experiments. In *Computer applications in fermentation technology modelling and control of biotechnological processes* (pp. 195–204). Amsterdam: Elsevier.

Nicolaï, B. M., van Impe, J. F., Martens, T., & de Baerdemaeker, J. (1995). A probabilistic model for microbial growth during cold storage of foods. In *Proceedings of the 19th international congress of refrigeration* (*vol. I*) (pp. 232–239). August, The Hague, The Netherlands.

Schouten, R. E., & van Kooten, O. (1998). Keeping quality of cucumber batches: Is it predictable? *Acta Horticulturae (Proceedings of the international symposium Model-It), 476*, 349–355.

Tijskens, L. M. M. (1990). *Champignon model*. Internal ATO report (in Dutch).

Tijskens, L. M. M., Hertog, M. L. A. T. M., van Kooten, O., & Simcic, M. (1999). Advantages of non-destructive measurements for understanding biological variance and for modelling the quality of perishable products. Deutsche Gesellschaft für Qualitätsforschung (Pflanzliche Nahrungsmittel) DGQ e.V. XXXIV. Vortragstagung, Zerstorungsfreie Qualitatsanalyse, Freising-Weihenstephan, Germany, 22–23 March 1999, pp. 13–23.

Tijskens, L. M. M., Otma, E. C., & van Kooten, O. (1998). Temperature effects in the rate constant of photosynthetic electron transport of cucumbers. In *COST915 Workshop physiological and technological aspects of gaseous and thermal treatments of fresh fruit and vegetables*. Madrid, 15–16 October 1998.

Tijskens, L. M. M., Rodis, P. S., Hertog, M. L. A. T. M., Kalantzi, U., & van Dijk, C. (1998). Kinetics of polygalacturonase activity and firmness of peaches during storage. *Journal of Food Engineering, 35*, 111–126.

Trelea, I. C., Trystram, G., & Courtois, F. (1997). Optimal constrained non-linear control of batch processes: Application to corn drying. *Journal of Food Engineering, 31*, 403–421.

Vankerschaver, K., Willocx, F., Smout, C., Hendrickx, M., & Tobback, P. (1996). Mathematical modelling of temperature and gas composition effects on visual quality changes in cut endive. *Journal of Food Science, 61*(3), 613–619.

Verdijck, G. J. C., & Lukasse, L. J. S. (2000). Control of quality evolution of agricultural products in climatised storage and transport using product quality evolution models. *Journal A, 41*(3), 37–43.

Verdijck, G. J. C., Weiss, M., & Preisig, H. A. (1999). Model-based product quality control for a potato storage facility. In *Proceedings of the American control conference* (pp. 2558–2562). San Diego, USA.